Transmission Expansion Planning using a Highly Accurate AC Optimal Power Flow Approximation

Otto Heide
University of Zagreb
Faculty of Electrical
Engineering and Computing
Zagreb, Croatia
Email: otto.heide@fer.hr

Karlo Šepetanc
University of Zagreb
Faculty of Electrical
Engineering and Computing;
Innovation Centre N. Tesla
Zagreb, Croatia
Email: karlo.sepetanc@fer.hr

Hrvoje Pandžić
University of Zagreb
Faculty of Electrical
Engineering and Computing;
Innovation Centre N. Tesla
Zagreb, Croatia
Email: hrvoje.pandzic@fer.hr

Abstract—The objective of transmission network expansion planning is to find the optimal strategy that balances the investment and the operating costs, considering all generation and transmission constraints. Attempts to address this problem in a tractable manner have led researchers to develop different convex relaxations and approximations. Due to the constant power grid evolution, new and improved approximation models are required to successfully handle the upcoming challenges. In this paper, we present a comprehensive approach to handle this highly complex problem both tractably and accurately. The model is based on a convex polar second-order Taylor expansion approximation of the AC power flows where both the voltage magnitudes and angles are quadratically constrained. The proposed approach achieves high accuracy due to the elimination of constraint relaxation errors, as determined by the presolve, which can occur due to the convexification process. The model demonstrated superior accuracy and similar computation times as the existing approximation models. In comparison to the exact formulations, our model shows similar accuracy while improving the computation time.

Index Terms—Optimal power flow approximation, transmission expansion planning, mixed-integer quadratically constrained quadratic program

Nomenclature

A. Sets and Indices

N	Set of buses, indexed by i and j.
N^P	Tuple set of paired buses aligned with branch E orientation, indexed by (i,j).
R	Set of reference buses, indexed by i.
E, E^R	Tuple set of branches, forward and reverse orientation, indexed by (e,i,j).
E_i, E_i^R	Array of tuple sets of branches at bus i, forward and reverse orientation, indexed by (e,i,j).
E^+, E^{R+}	Tuple set of prospective expansion branches, forward and reverse orientation, indexed by (e,i,j).
$E_i{}^+, E_i^{R+}$	Array of tuple sets of prospective expansion branches at bus i, forward and reverse orientation, indexed by (e,i,j).
G, G_i	Set of all generators and array of sets of generators at bus i, indexed by k.
L_i	Array of sets of loads at bus i, indexed by l.
S_i	Array of sets of shunts at bus i, indexed by s.
τ	Set of time steps, indexed by t.
Ω, Ω_i	Set of all wind generators and array of sets of wind generators at bus i, indexed by w.
Ξ	Set of decision variables.

B. Parameters

$\ddot{c}_k, \dot{c}_k, c_k$	Generator cost coefficients.
$P_{t,l}^{\mathrm{d}}, Q_{t,l}^{\mathrm{d}}$	Active and reactive power load.
$g_s^{\mathrm{sh}}, b_s^{\mathrm{sh}}$	Bus shunt conductance and susceptance.
$g_e, g_e^{\mathrm{fr}}, g_e^{\mathrm{to}}$	Branch π-section conductances.
$b_e, b_e^{\mathrm{fr}}, b_e^{\mathrm{to}}$	Branch π-section susceptances.
τ_e, σ_e	Branch tap magnitude and shift angle.
$\underline{P}_k^{\mathrm{g}}, \overline{P}_k^{\mathrm{g}}$	Generator minimum and maximum active power output.
$\underline{Q}_k^{\mathrm{g}}, \overline{Q}_k^{\mathrm{g}}$	Generator minimum and maximum reactive power output.
$\overline{P}_w^{\omega}$	Wind generator maximum active power output.
$\overline{S}_e$	Branch maximum apparent power.
$\underline{\theta}_{i,j}, \overline{\theta}_{i,j}$	Bus-pair minimum and maximum voltage angle difference.
$\underline{V}_i, \overline{V}_i$	Bus minimum and maximum voltage magnitude.
$V_{t,i}^{\mathrm{op}}, \theta_{t,i}^{\mathrm{op}}$	Assumed bus voltage magnitude and angle operating points.
$\Lambda_{t,e}, \Gamma_{t,i,j}$	Boolean parameters which indicate whether to use quadratic form of voltage and cosine representation respectively.
M	Disjunctive factor, a large positive number.
$cost_e$	Expansion cost coefficient.

C. Variables

$P_{t,k}^{\mathrm{g}}, Q_{t,k}^{\mathrm{g}}$	Generator active and reactive power production.
$P_{t,w}^{\omega}$	Wind generator active power production.
$P_{t,e,i,j}, Q_{t,e,i,j}$	Branch active and reactive power flow.
$V_{t,i}^{\Delta}, \theta_{t,i}^{\Delta}$	Bus voltage magnitude and angle change.
$V_{t,i}, \theta_{t,i}$	Bus voltage and magnitude.
$\widehat{cos}_{t,i,j}$	Cosine approximation.
$\check{V}_{t,e}$	Second order Taylor series voltage magnitude term approximation.
z_e	Binary decision variable for a prospective line.

1. INTRODUCTION

A. Motivation and background

Transmission expansion planning (TEP) represents an important research area in the field of power systems. TEP determines the location and number of new lines that need to be installed to achieve certain goals in the transmission of electrical power. An optimal TEP solution usually consists of several targets, such as increasing reliability and ensuring the security of supply, minimizing the investment and operating costs, reducing power losses, and avoiding potential congestion. With the continuous increase in demand levels, more lines will become congested in the near future and for that reason, it is important to identify and improve potential weak spots in the transmission system to ensure system security and to maximize social welfare.

The nonlinear and non-convex nature of the exact AC TEP problem makes the computation of the globally optimal solution, in a reasonable time, difficult to achieve, especially when large-scale networks are considered. The TEP problem has been solved using mathematical optimization approximation and relaxation models [1] – [11] and heuristic optimization methods [12] – [14]. Paper [15] presents a comprehensive review and classification of available publications and models on the TEP problem. Heuristic methods, based on the power flow results, incrementally select expansion line that removes congestion in a selected part of the network. Considering the added line, power flow analysis is recalculated and the process continues step-by-step until there is no more congestion in the network. Heuristic methods rarely achieve global optimality and do not provide any optimality estimates. On the other hand, convex mathematical optimization models provide model's solution optimality guarantees, but no feasibility guarantees due to reduced accuracy due to applied relaxations or approximations. Several methods have been proposed for the TEP problem and they mostly use classical optimization techniques, such as linear programming [3] – [5], non-linear programming [6] and mixed-integer programming [7] – [8].

B. Literature review

Due to the high computational complexity of TEP, using one of the exact AC network models is not a popular approach despite the ultimate accuracy of the obtained solution. Thus, [12] presented a mixed-integer nonlinear programming (MINLP) approach for solving TEP for an AC network model using heuristic algorithms and interior point method which obtained a quality solution for the presented problem. For mathematical optimization programming, approximations such as linear DC model [10], piecewise-linearized AC model [1] and linear-programming of AC power flows (LPAC) [9] are commonly used to approximate the exact AC power flow equations.

The DC model approximation has the fastest computation time compared to any other approach, but in terms of accuracy, it results in a suboptimal and frequently infeasible solution in reality. Accuracy gap of the linear DC model compared to the exact one arises from simplifications made when neglecting

reactive power flows, active power losses, and voltage drops in network optimization modeling [2], [12], [14]. Piecewise linearization of AC power flows (LACTEP) was introduced in [1], where reactive power flows, active power losses, and off-nominal bus voltage magnitudes were retained. Linearization is based on the first-order Taylor series expansion and is used to separately model network losses initially defined as non-convex constraints. The optimal solution and computation time highly correlate with the number of linear blocks used in the piecewise linearization process. The objective function in this approach varies with the number of linear blocks. To obtain the best solution, it is necessary to perform an iterative sensitivity analysis with different number of linear blocks, which results in a prolonged computation time. [9] proposes a linear approximation of the AC power flow equations (LPAC) that, contrary to the DC model, captures reactive power flows and voltage magnitudes, as well as active and reactive power losses, which means they do not have to be modeled separately as in [1]. The linearity of power flow equations in the LPAC model is highly desirable in terms of computational tractability. However, for the TEP process, the cosine approximation is modeled in its quadratically constrained formulation to better capture the voltage angle variable, thus the LPAC model in this paper is presented as a mixed-integer quadratically constrained quadratic programming (MIQCQP) model.

However, all of the previously mentioned popular approximations tend to have certain accuracy disadvantages when it comes to modeling of reactive power flows, voltage magnitudes, and losses, and thus often result in a suboptimal or even infeasible solutions. On the other hand, convex quadratic approaches of the AC power flows can achieve high accuracy when there are no constraint relaxation errors due to the convexification process. A new ACOPF approximation approach [16] is based on the convex polar second-order Taylor approximation (CPSOTA) of AC power flows, where the relaxed quadratic constraints that would likely cause relaxation errors are identified in the presolve process. The identified quadratic inequalities are substituted with linear equality constraints, significantly improving model's accuracy. Our work builds upon the CPSOTA approximation by introducing new constraints necessary for TEP.

C. Paper contribution and structure

Contribution of the paper consists of the following:

- We present new model for TEP process based on the Taylor series that approximates second-order voltage variables.
- Presolve technique is used to decide whether to use the quadratic or the linear form of power flow constraints to avoid constraint relaxation errors due to the convexification process.
- The resulting MIQCQP solution is obtained much quicker than the MINLP solution, while maintaining high accuracy

Rest of the paper is structured as follows: Section 2 presents our mathematical model for TEP problem. Subsection 2 -A in-

troduces the presolve technique and Subsection 2 -B presents model components. Case study is presented in Section 3 . It presents description and set-up of test cases, and algorithm that describes four step procedure of our TEP model. Section 4 provides relevant conclusions and guidelines for future work.

2 . MATHEMATICAL MODEL

Our model is based on the convex polar second-order Taylor approximation of AC power flows where both the voltage magnitudes and angles are quadratically constrained. The proposed approach achieves high accuracy due to the elimination of constraint relaxation errors, as determined in the presolve process, which can occur due to the convexification process. Detailed algorithmic implementation of the presented model is defined in Section 3 .

A. Presolve technique

The convex quadratic approach can achieve high accuracy when there are no constraint relaxation errors that result from the convexification process. The presolve process identifies constraints that would likely cause relaxation errors and decides whether to use the quadratic or the linear form of power flow constraints to avoid relaxation errors.

$$
\check{V}_{t,e} = \frac{g_e + g_e^{\mathbf{fr}}}{\tau_e^2} \cdot (V_{t,i}^{\Delta})^2 - \frac{2 \cdot g_e}{\tau_e} \cdot \cos(\theta_{t,i}^{\mathbf{op}} - \theta_{t,j}^{\mathbf{op}} - \sigma_e) \cdot V_{t,i}^{\Delta} \cdot V_{t,j}^{\Delta}
$$
$$
+ (g_e + g_e^{\mathbf{to}}) \cdot (V_{t,j}^{\Delta})^2, \quad \forall t, (e,i,j) \in E \quad (1.1)
$$

$$
\widehat{cos}_{t,i,j} = 1 - \frac{(\theta_{t,i}^{\Delta} - \theta_{t,j}^{\Delta})^2}{2}, \quad \forall t, (i,j) \in N^{\mathrm{P}} \quad (1.2)
$$

Swapping the inequality constraints in equations (2.8) and (2.10) with their linear alternative in equations (2.9) and (2.11) avoids constraint relaxation errors due to convexification process. The decision for swapping inequality constraints with their linear alternative is based on the marginal value of equations (1.1) and (1.2), which are defined as quadratic equality constraints in the presolve process. Constraints' marginal values represent the sensitivity of the objective function on these constraints and they are computed by default by many solvers, e.g. IPOPT. For constraint (2.8) to be binding, due to its greater-or-equal sign, $\check{V}_{t,e}$ should have the tendency to be as small as possible, i.e. marginal value of (1.1) needs to be positive. Oppositely, for constraint (2.10) to be binding, due to its less-or-equal sign, marginal value of (1.2) needs to be negative. Therefore, the quadratic form of constraint $\check{V}_{t,e}$ is used only if the Boolean parameter $\Lambda_{t,e}$ is true and conductance g_e is positive, and quadratic form of constraint $\widehat{cos}_{t,i,j}$ is used only in the Boolean parameter $\Gamma_{t,i,j}$ is true.

B. Optimization model

This subsection presents the whole network-constrained TEP model.

$$
\mathrm{Min}(\sum_{t,k}(\ddot{c}_k \cdot (P_{t,k}^{\mathrm{g}})^2 + \dot{c}_k \cdot P_{t,k}^{\mathrm{g}} + c_k) + \sum_{e \in E^+} z_e \cdot cost_e) \quad (2.1)
$$

$$
\sum_{k \in G_i} P_{t,k}^{\mathrm{g}} - \sum_{l \in L_i} \boldsymbol{P}_{t,l}^{\mathbf{d}} - \sum_{(e,i,j) \in E_i \cup E_i^{\mathrm{R}}} P_{t,e,i,j} - \sum_{(e,i,j) \in (E_i^+ \cup E_i^{\mathrm{R}+})} P_{t,e,i,j}
$$
$$
- ((V_{t,i}^{\mathbf{op}})^2 + 2 \cdot V_{t,i}^{\mathbf{op}} \cdot V_{t,i}^{\Delta}) \cdot \sum_{s \in S_i} \boldsymbol{g}_s^{\mathbf{sh}} + \sum_{w \in \Omega} P_{t,w}^{\omega} = 0, \forall t, i
$$
$$
(2.2)
$$

$$
\sum_{k \in G_i} Q_{t,k}^{\mathrm{g}} - \sum_{l \in L_i} \boldsymbol{Q}_{t,l}^{\mathbf{d}} - \sum_{(e,i,j) \in E_i \cup E_i^{\mathrm{R}}} Q_{t,e,i,j} - \sum_{(e,i,j) \in (E_i^+ \cup E_i^{\mathrm{R}+})} Q_{t,e,i,j}
$$
$$
+ ((V_{t,i}^{\mathbf{op}})^2 + 2 \cdot V_{t,i}^{\mathbf{op}} \cdot V_{t,i}^{\Delta}) \cdot \sum_{s \in S_i} \boldsymbol{b}_s^{\mathbf{sh}} = 0, \quad \forall t, i \quad (2.3)
$$

$$
P_{t,e,i,j} = \frac{((V_{t,i}^{\mathbf{op}})^2 + 2 \cdot V_{t,i}^{\mathbf{op}} \cdot V_{t,i}^{\Delta}) \cdot (g_e + g_e^{\mathbf{fr}})}{\tau_e^2} + \frac{\check{V}_{t,e}}{2}
$$
$$
- (g_e \cdot \cos(\theta_{t,i}^{\mathbf{op}} - \theta_{t,j}^{\mathbf{op}} - \sigma_e) + b_e \cdot \sin(\theta_{t,i}^{\mathbf{op}} - \theta_{t,j}^{\mathbf{op}} - \sigma_e)) \cdot
$$
$$
(V_{t,i}^{\mathbf{op}} \cdot V_{t,j}^{\mathbf{op}} \cdot \widehat{cos}_{t,i,j} + V_{t,i}^{\Delta} \cdot V_{t,j}^{\mathbf{op}} + V_{t,j}^{\Delta} \cdot V_{t,i}^{\mathbf{op}}) / \tau_e
$$
$$
- (b_e \cdot \cos(\theta_{t,i}^{\mathbf{op}} - \theta_{t,j}^{\mathbf{op}} - \sigma_e) - g_e \cdot \sin(\theta_{t,i}^{\mathbf{op}} - \theta_{t,j}^{\mathbf{op}} - \sigma_e)) \cdot
$$
$$
V_{t,i}^{\mathbf{op}} \cdot V_{t,j}^{\mathbf{op}} \cdot (\theta_{t,i}^{\Delta} - \theta_{t,j}^{\Delta}) / \tau_e, \quad \forall t, (e,i,j) \in E \quad (2.4)
$$

$$
P_{t,e,i,j} = ((V_{t,i}^{\mathbf{op}})^2 + 2 \cdot V_{t,i}^{\mathbf{op}} \cdot V_{t,i}^{\Delta}) \cdot (g_e + g_e^{\mathbf{to}}) + \frac{\check{V}_{t,e}}{2}
$$
$$
- (g_e \cdot \cos(\theta_{t,i}^{\mathbf{op}} - \theta_{t,j}^{\mathbf{op}} + \sigma_e) + b_e \cdot \sin(\theta_{t,i}^{\mathbf{op}} - \theta_{t,j}^{\mathbf{op}} + \sigma_e)) \cdot
$$
$$
(V_{t,i}^{\mathbf{op}} \cdot V_{t,j}^{\mathbf{op}} \cdot \widehat{cos}_{t,j,i} + V_{t,i}^{\Delta} \cdot V_{t,j}^{\mathbf{op}} + V_{t,j}^{\Delta} \cdot V_{t,i}^{\mathbf{op}}) / \tau_e
$$
$$
- (b_e \cdot \cos(\theta_{t,i}^{\mathbf{op}} - \theta_{t,j}^{\mathbf{op}} + \sigma_e) - g_e \cdot \sin(\theta_{t,i}^{\mathbf{op}} - \theta_{t,j}^{\mathbf{op}} + \sigma_e)) \cdot
$$
$$
V_{t,i}^{\mathbf{op}} \cdot V_{t,j}^{\mathbf{op}} \cdot (\theta_{t,i}^{\Delta} - \theta_{t,j}^{\Delta}) / \tau_e, \quad \forall t, (e,i,j) \in E^{\mathrm{R}} \quad (2.5)
$$

$$
Q_{t,e,i,j} = - \frac{((V_{t,i}^{\mathbf{op}})^2 + 2 \cdot V_{t,i}^{\mathbf{op}} \cdot V_{t,i}^{\Delta}) \cdot (b_e + b_e^{\mathbf{fr}})}{\tau_e^2}
$$
$$
+ (b_e \cdot \cos(\theta_{t,i}^{\mathbf{op}} - \theta_{t,j}^{\mathbf{op}} - \sigma_e) - g_e \cdot \sin(\theta_{t,i}^{\mathbf{op}} - \theta_{t,j}^{\mathbf{op}} - \sigma_e)) \cdot
$$
$$
(V_{t,i}^{\mathbf{op}} \cdot V_{t,j}^{\mathbf{op}} \cdot \widehat{cos}_{t,i,j} + V_{t,i}^{\Delta} \cdot V_{t,j}^{\mathbf{op}} + V_{t,j}^{\Delta} \cdot V_{t,i}^{\mathbf{op}}) / \tau_e
$$
$$
- (g_e \cdot \cos(\theta_{t,i}^{\mathbf{op}} - \theta_{t,j}^{\mathbf{op}} - \sigma_e) + b_e \cdot \sin(\theta_{t,i}^{\mathbf{op}} - \theta_{t,j}^{\mathbf{op}} - \sigma_e)) \cdot
$$
$$
V_{t,i}^{\mathbf{op}} \cdot V_{t,j}^{\mathbf{op}} \cdot (\theta_{t,i}^{\Delta} - \theta_{t,j}^{\Delta}) / \tau_e, \quad \forall t, (e,i,j) \in E
$$
$$
(2.6)
$$

$$
Q_{t,e,i,j} = - ((V_{t,i}^{\mathbf{op}})^2 + 2 \cdot V_{t,i}^{\mathbf{op}} \cdot V_{t,i}^{\Delta}) \cdot (b_e + b_e^{\mathbf{to}})
$$
$$
+ (b_e \cdot \cos(\theta_{t,i}^{\mathbf{op}} - \theta_{t,j}^{\mathbf{op}} + \sigma_e) - g_e \cdot \sin(\theta_{t,i}^{\mathbf{op}} - \theta_{t,j}^{\mathbf{op}} + \sigma_e)) \cdot
$$
$$
(V_{t,i}^{\mathbf{op}} \cdot V_{t,j}^{\mathbf{op}} \cdot \widehat{cos}_{t,j,i} + V_{t,i}^{\Delta} \cdot V_{t,j}^{\mathbf{op}} + V_{t,j}^{\Delta} \cdot V_{t,i}^{\mathbf{op}}) / \tau_e
$$
$$
- (g_e \cdot \cos(\theta_{t,i}^{\mathbf{op}} - \theta_{t,j}^{\mathbf{op}} + \sigma_e) + b_e \cdot \sin(\theta_{t,i}^{\mathbf{op}} - \theta_{t,j}^{\mathbf{op}} + \sigma_e)) \cdot
$$
$$
V_{t,i}^{\mathbf{op}} \cdot V_{t,j}^{\mathbf{op}} \cdot (\theta_{t,i}^{\Delta} - \theta_{t,j}^{\Delta}) / \tau_e, \quad \forall t, (e,i,j) \in E^{\mathrm{R}} \quad (2.7)
$$

$$
\check{V}_{t,e} \geqslant \frac{g_e + g_e^{\mathbf{fr}}}{\tau_e^2} \cdot (V_{t,i}^{\Delta})^2 - \frac{2 \cdot g_e}{\tau_e} \cdot \cos(\theta_{t,i}^{\mathbf{op}} - \theta_{t,j}^{\mathbf{op}} - \sigma_e) \cdot V_{t,i}^{\Delta} \cdot V_{t,j}^{\Delta}
$$
$$
+ (g_e + g_e^{\mathbf{to}}) \cdot (V_{t,j}^{\Delta})^2, \quad \forall t, (e,i,j) \in (E \cup E^+) : g_e > 0 \wedge \Lambda_{t,e}
$$
$$
(2.8)
$$

$$
\check{V}_{t,e} = 0, \quad \forall t, (e,i,j) \in (E \cup E^+) : g_e \leqslant 0 \vee \neg \Lambda_{t,e} \quad (2.9)
$$

$$
\widehat{cos}_{t,i,j} \leqslant 1 - \frac{(\theta_{t,i}^{\Delta} - \theta_{t,j}^{\Delta})^2}{2}, \quad \forall t, (i,j) \in N^{\mathrm{P}} : \Gamma_{t,i,j} \quad (2.10)
$$

$$
\widehat{cos}_{t,i,j} = 1, \quad \forall t, (i,j) \in N^{\mathrm{P}} : \neg \Gamma_{t,i,j} \quad (2.11)
$$

$$
0 \leqslant P_{t,w}^{\omega} \leqslant \overline{\boldsymbol{P}}_w^{\omega}, \quad \forall t, w \quad (2.12)
$$

$$
\underline{\boldsymbol{P}}_k^{\mathbf{g}} \leqslant P_{t,k}^{\mathrm{g}} \leqslant \overline{\boldsymbol{P}}_k^{\mathbf{g}}, \quad \forall t, k \quad (2.13)
$$

$$\underline{\boldsymbol{Q}}^{\mathbf{g}}_k \leqslant Q^{\mathrm{g}}_{t,k} \leqslant \overline{\boldsymbol{Q}}^{\mathbf{g}}_k, \quad \forall t, k \qquad (2.14)$$

$$P^2_{t,e,i,j} + Q^2_{t,e,i,j} \leqslant \overline{\boldsymbol{S}}^2_e, \quad \forall t, (e,i,j) \in (E \cup E^{\mathrm{R}}) : \exists \overline{\boldsymbol{S}}_e \qquad (2.15)$$

$$\boldsymbol{\theta}^{\mathbf{op}}_{t,i} + \theta^{\Delta}_{t,i} = 0, \quad \forall t, i \in R \qquad (2.16)$$

$$\underline{\boldsymbol{V}}_i \leqslant \boldsymbol{V}^{\mathbf{op}}_{t,i} + V^{\Delta}_{t,i} \leqslant \overline{\boldsymbol{V}}_i, \quad \forall t, i \qquad (2.17)$$

$$\underline{\boldsymbol{\theta}}_{i,j} \leqslant (\boldsymbol{\theta}^{\mathbf{op}}_{t,i} + \theta^{\Delta}_{t,i}) - (\boldsymbol{\theta}^{\mathbf{op}}_{t,j} - \theta^{\Delta}_{t,j}) \leqslant \overline{\boldsymbol{\theta}}_{i,j}, \forall t, (i,j) \in N^{\mathrm{P}} \qquad (2.18)$$

$$(z_e - 1) \cdot M \leqslant P_{t,e,i,j} - p_f(\psi) \leqslant (1 - z_e) \cdot M, \forall e \in E^{+} \qquad (2.19)$$

$$(z_e - 1) \cdot M \leqslant P_{t,e,i,j} - p_t(\psi) \leqslant (1 - z_e) \cdot M, \forall e \in E^{\mathrm{R}+} \qquad (2.20)$$

$$(z_e - 1) \cdot M \leqslant Q_{t,e,i,j} - q_f(\psi) \leqslant (1 - z_e) \cdot M, \forall e \in E^{+} \qquad (2.21)$$

$$(z_e - 1) \cdot M \leqslant Q_{t,e,i,j} - q_t(\psi) \leqslant (1 - z_e) \cdot M, \forall e \in E^{\mathrm{R}+} \qquad (2.22)$$

$$P^2_{t,e,i,j} + Q^2_{t,e,i,j} \leqslant \overline{\boldsymbol{S}}^2_e \cdot z_e, \forall t, (e,i,j) \in (E^{+} \cup E^{\mathrm{R}+}) : \exists \overline{\boldsymbol{S}}_e \qquad (2.23)$$

The objective function (2.1) minimizes total operating and investment cost over defined time period. For operating cost we use quadratic cost curve. Equations (2.2) and (2.3) represent bus balance constraints for active and reactive power. Constraints (2.4)–(2.7) represent power flow equations for existing lines which also contain second-order term approximation variables $\check{V}_{t,e}$ and $\boldsymbol{\theta}^{\mathbf{op}}_{t,i}$ that are defined from (2.8) - (2.11). Wind generators output is limited by its maximum generating capacity as defined in (2.12), and output limits of active and reactive power for conventional generators are set in (2.13) and (2.14). Constraint (2.15) defines maximum branch apparent power flow in both directions. Equation (2.16) defines the reference bus angle value. Voltage magnitude and bus-pair angle constraints are defined in (2.17) and (2.18). Constraints (2.19)–(2.22) represent power flow equations for prospective lines, where $p_f(\psi)$, $p_t(\psi)$, $q_f(\psi)$, $q_t(\psi)$ are sequentially defined as the right-hand side of equations (2.4)–(2.7). Equation (2.23) is used to force the power flow on prospective lines to be equal to zero it the prospective line is not selected for the expansion process.

3. CASE STUDY

We demonstrate the accuracy of our model on the IEEE 24-bus and the IEEE 73-bus (RTS96) systems from the OPF benchmark [17]. Due to the limited amount of available network data for transmission network expansion planning, the presented grids are modified to capture different time intervals during the operating horizon. Wind power generation units are included in the system, and their active power production limits are defined for each time step, which have assigned occurrence frequency throughout the target years. Detailed input data on these modified power systems can be found in [18]. To incur congestion, conventional generator's minimum production limits are reduced by the factor of 50% and the line ratings are reduced by the factor of 20% as compared to the original values defined in [17]. Different time segments are used to account for different branch power flows that occur as a result of variable output of wind generator active power production at each time period. Therefore, during the different
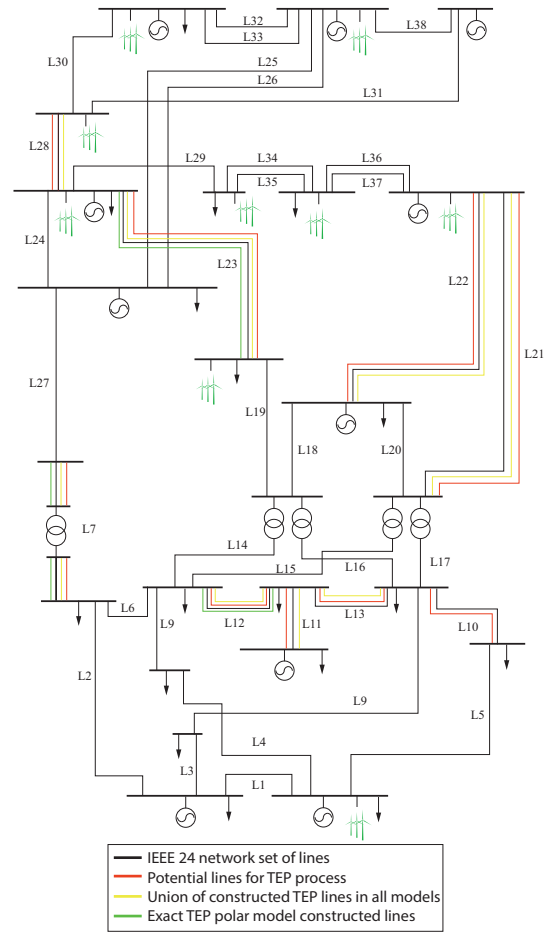
Fig. 1: IEEE 24-bus system for TEP.

time segments, different lines are identified as prospective candidates for the expansion of the transmission network. For the IEEE 24-bus system, the number of representative time steps is set to 7, and for the IEEE 73-bus (RTS96) system it is set to 5. The IEEE 73-bus (RTS96) system with 120 branches is a complex network by itself. To capture a computationally complex, yet time feasible case study, the number of prospective candidate lines for the IEEE 24-bus system with 38 branches has to be greater than for the IEEE 73-bus (RTS96) system. Set of prospective expansion branches E_i^{+} is determined after the first step of our model where the lines with the apparent flow greater than 70% of their capacity, for the IEEE 24-bus system, are defined as prospective candidates. For the IEEE 73-bus (RTS96) system, lines with the apparent flow value greater than 90% of their capacity are chosen as prospective candidates. It is assumed that at most one line is allowed to be added in each transmission corridor in the TEP process. The IEEE 24-bus system with prospective and constructed lines is visualized in Fig. 1.

The accuracy of the presented model is obtained through a four-step process. Our computation procedure starts with the exact AC polar model where the network expansion binary variables are excluded. This step provides a good Taylor expansion operating point of both the voltage magnitude and

angle, which are then used in the second step. The second step is defined as a presolve where the non-convex form of our model is run, but also without the computationally demanding binary variables. In the non-convex form, quadratic inequality constraints (2.8) and (2.10) are applied as quadratic equality constraints (1.1) and (1.2) whose marginal value signs we use to determine if the constraint would be binding if relaxed, as described in Subsection 2 -A. The third step is to run the main, full mixed-integer AC TEP using the convex approximation around the previously computed operating point, with binary variables and constraints defined in the presolve. The last step is to run the exact polar model where binary variables are considered as parameters whose values are defined in the previous step. Results of this step will determine approximation errors that were made in this model. The described procedure is itemized in Algorithm 1.

Algorithm 1 Transmission expansion planning (TEP)

1: Run exact polar model without binary variables for transmission expansion (NLP)
2: Run non-convex presolve using the operating point from the previous step, also without binary variables for transmission expansion (non-convex QCQP)
{In this step the presolve selects constraints for the main TEP computation by evaluating the constraints' marginal value}
3: Run the main TEP model around the previously computed operating point with binary variables for transmission expansion (MIQCQP)
4: Run the exact polar model with fixed binary variables to TEP solution in step 3 to determine approximation error (NLP)

Simulation results are provided in Table I and Table II, and their visual representation is provided in Fig 2. and Fig 3.

Our convex approximation (CPSOTA) is compared with the exact AC polar model, linearized AC model (LPAC) [9], linear DC model, Jabr's relaxed second-order cone programming model (JABR) [19] and piecewise-linearized AC model (LACTEP) [1].

In both test cases, the presented model by far outperforms other approximations in terms of the objective function value error and, more importantly, it is the only one that yields the correct expansion plan. Construction of the new transmission

Fig. 2: Visualization of different TEP models accuracy for the IEEE 24-bus system test case.
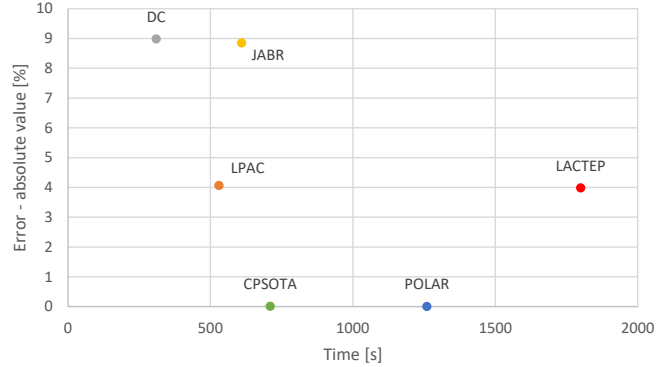
Fig. 3: Visualization of different TEP models accuracy for the IEEE 73-bus system test case.

power lines shifts the cost from operation to investment, but eventually, TEP process provides saving in total costs. Due to imprecise modeling of the reactive power flows, voltage magnitudes and power losses, the LPAC, JABR, and LACTEP models do not accurately reflect the actual solution, thus those models in both test cases result in expansion plans that consists of larger sets of newly erected lines than the exact AC polar model. The larger expansion plan of those models results in lower, realistically imprecise, total costs. Consequently, the approximation error of those models is greater than of the proposed CPSOTA model that captures the same expansion plan as the exact AC polar model. The

TABLE I
TEP RESULT COMPARISON FOR THE IEEE 24-BUS SYSTEM

Model	Time [s]	Expansion plan	Total cost	Error [%]
POLAR (MINLP)	2730	L7, L13, L23	4.0359299 E+09	0
LPAC (MIQCQP)	240	L7, L12, L13 L21, L22, L23, L28	3.9130797 E+09	-3.044
DC (MILP)	70	L12, L22, L23, L28	3.7468042 E+09	-7.164
JABR's (MISOCP)	130	L7, L12, L13 L21, L22, L23, L28	3.9138228 E+09	-3.026
LACTEP (MILP)	370	L7, L11, L12, L13 L21, L22, L23, L28	3.9116847 E+09	-3.078
CPSOTA (MIQCQP)	340	L7, L13, L23	4.0361073 E+09	0.004

TABLE II
TEP RESULT COMPARISON FOR THE IEEE 73-BUS (RTS96) SYSTEM

Model	Time [s]	Expansion plan	Total cost	Error [%]
POLAR (MINLP)	1260	L30, L90	1.390911 E+10	0
LPAC (MIQCQP)	530	L25, L53, L91, L102	1.334429 E+10	-4.061
DC (MILP)	310	L53	1.265998 E+10	-8.981
JABR's (MISOCP)	610	L30, L53 L69, L90, L91	1.267801 E+10	-8.851
LACTEP (MILP)	1800	L25, L53 L69, L90, L91	1.335497 E+10	-3.984
CPSOTA (MIQCQP)	710	L30, L90	1.390794 E+10	-0.008

DC model determines a larger set of required lines than the exact AC polar model for the expansion process of the IEEE 24-bus system, which has a large set of prospective candidates. On the other hand, the DC model for the IEEE 73-bus (RTS96) system captures a smaller set of required lines than the exact AC polar model. As expected, in both test cases the linear DC model has the highest approximation error. Computation-time-wise, the presented CPSOTA model is faster than LACTEP approximation and slower than JABR's relaxation, and DC and LPAC approximations for both test cases. The highest objective function approximation error of the CPSOTA model, in both test cases, is -0.008% as compared to the exact AC polar model. In terms of the total computation time, the CPSOTA model is 87% faster than the exact AC polar model for the IEEE 24-bus system with a larger set of prospective lines. For the IEEE 73-bus (RTS96) system, with a smaller set of prospective lines, the CPSOTA model achieves 43% faster total computation time than the exact AC polar model. The presented model is accurate around the operating point estimated by solving the exact AC polar model without binary variables for transmission expansion. The advantage of this approach is the possibility to iteratively run the main TEP model by updating the operating point and retesting the constraints in step 2 of Algorithm 1 for that new operating point. This way the approximation errors reduce even further.

4. Conclusion

This paper utilizes the recently published convex polar second-order Taylor approximation of AC power flows [16] to deliver high modeling accuracy and tractability to the TEP. Model's accuracy is achieved by utilization of quadratically constrained voltage magnitudes and angles. In the presolve process quadratic inequality constraints, which could cause relaxation errors due to the convexification process, are identified and replaced by their linear equality constraint alternative. The method is evaluated on two modified test cases based on the PGLib-OPF benchmark [17] and compared against the existing models. The proposed model demonstrates superior accuracy at no additional computation cost, as computation times are similar to the ones achieved by using the existing approximation models. In comparison to the exact AC power flow formulations, our model shows similar accuracy and the same realistic expansion planning results, while computation time is significantly improved. The high accuracy of the presented model is desirable for further applications in more complex power systems with flexible devices, such as battery energy storage systems (BESS). The BESS will have an important role in congestion reduction, voltage control, and transition to the sustainable and secure energy system based on renewable sources. The BESS can be favorable at locations where construction of new lines is not possible, and to reduce power curtailment at locations where renewable energy sources are installed. It is also possible to coordinate TEP with the generation expansion planning (GEP) by allocating the necessary expansion investments. However, the selection of different generation units for the expansion process can affect the TEP results. The relationship between TEP and GEP can be investigated in the future work.

References

[1] H. Zhang, G. T. Heydt, V. Vittal and J. Quintero, "An Improved Network Model for Transmission Expansion Planning Considering Reactive Power and Network Losses," *IEEE Trans. Power Syst.*, vol. 28, no. 3, pp. 3471–3479, Aug. 2013.

[2] J. Jundi, "Transmission Expansion Planning in Large Power Systems Using Power System Equivalencing Techniques," 2014.

[3] R. S. Chanda and P. K. Bhattacharjee, "Application of Computer Software in Transmission Expansion Planning Using Variable Load Structure," *Electric Power System Research*, no. 31, pp. 13–20, 1994.

[4] R. Villasana, L. L. Garver and S.L. Salon, "Transmission Network Planning Using Linear Programming," *IEEE Trans. Power Apparat. Syst.*, vol. PAS-104, pp. 349–356, Feb. 1985.

[5] L. L. Garver, "Transmission Network Estimation Using Linear Programming," *IEEE Trans. Power Apparat. Syst.*, vol. PAS-89, pp. 1688–1697, Sept./Oct. 1970.

[6] H. K. Youssef and R. Hackaam, "New Transmission Planning Model," *IEEE Trans. Power Syst.*, vol. 4, pp. 9–18, Feb. 1989.

[7] L. Bahiense, G. C. Oliveira, M. Pereira and S. Granville, "A Mixed-Integer Disjunctive Model for Transmission Network Expansion," *IEEE Trans. Power Syst.*, vol. 16, pp. 560–565, Aug. 2001.

[8] S. T. Lee, K. L. Hocks, and E. Hnyilicza, "Transmission Expansion Using Branch-and-Bound Integer Programming with Optimal Cost-Capacity Curves," *IEEE Trans. Power Apparat. Syst.*, vol. PAS-93, pp. 1390–1400, July. 1974.

[9] C. Coffrin and P. Van Hentenryck, "A Linear-Programming Approximation of AC Power Flows," *INFORMS Journal on Computing*, 2012.

[10] R. Romero, A. Monticelli, A. Garcia and S. Haffner, "Test Systems and Mathematical Models for Transmission Network Expansion Planning," *IEE Proc., Gen. Trans. Distrib.*, vol. 149, (1), pp. 27–36., 2002.

[11] Z. Luburić, H. Pandžić and M. Carrion, "Test Systems and Mathematical Models for Transmission Network Expansion Planning,"Transmission Expansion Planning Model Considering Battery Energy Storage, TCSC and Lines Using AC OPF," *IEEE Access*, vol. 8, pp. 203429–203439., Jan. 2020.

[12] M. J. Rider, A. V. Garcia and R. Romero, "Power System Transmission Network Expansion Planning Using AC Model," *IET Gener. Transm. Distrib.*, vol. 1, no. 5, Sep. 2007.

[13] R. Bent, G. L. Toole and A. Berscheid, "Transmission Network Expansion Planning With Complex Power Flow Models," *IEEE Trans. Power Syst.*, vol. 27, no. 2, pp. 904–912, May. 2012.

[14] R. Bent, C. Coffrin, R. Gumucio and P. Van Hentenryck, "Transmission Network Expansion Planning: Bridging the Gap between AC Heuristics and DC Approximations," *Power Systems Computation Conference, Wroclaw*, 2014., pp. 1-8.

[15] G. Latorre, R. D. Cruz, J. M. Areiza and A. Villegas, "Classification of Publications and Models on Transmission Expansion Planning," *IEEE Trans. Power Syst.*, vol. 18, no. 2, pp. 938–946, May. 2003.

[16] K. Šepetanc and H. Pandžić, "Convex Polar Second-Order Taylor Approximation of AC Power Flows: A Unit Commitment Study," *IEEE Trans. Power Syst.*, Dec. 2020, Early Access.

[17] C. Coffrin *et al. PGLib-OPF*, GitHub, July 29, 2020. Accessed on: Jan. 9, 2021. [Online] Available at: github.com/power-grid-lib/pglib-opf/

[18] H. Pandžić, Y. Dvorkin, T. Qiu, Y. Wang and D. S. Kirschen, "Unit Commitment Under Uncertainty - GAMS Models," *REAL Lab Library*, University of Washington, Seattle, WA, USA. Accessed: March. 2021., [Online] Avalilable at: http://labs.ece.uw.edu/real/gams_code.html

[19] D. K. Molzahn and I. A. Hiskens, "A Survey of Relaxations and Approximations of the Power Flow Equations," pp. 75–77, 2019.